Long non-coding RNA H19 protects H9c2 cells against hypoxia-induced injury by activating the PI3K/AKT and ERK/p38 pathways

LINHUI YUAN[1*], LEITAO YU[2*], JING ZHANG[1], ZHIDONG ZHOU[1], CHANG LI[1], BIN ZHOU[1], XIAOLAN HU[1], GUOHAI XU[1] and YANHUA TANG[3]

Departments of [1]Anesthesiology, [2]Thyroid Surgery and [3]Cardiac Surgery, The Second Affiliated Hospital of Nanchang University, Nanchang, Jiangxi 330006, P.R. China

Received December 5, 2018; Accepted July 12, 2019

DOI: 10.3892/mmr.2020.10978

Abstract. Myocardial ischemia/reperfusion injury often leads to adverse cardiovascular outcomes due to severe hypoxia. The present study aimed to evaluate the effects and mechanism of long non-coding RNA H19 (H19) on rat H9c2 cells with hypoxia-induced injury. H9c2 cells were infected with lentiviruses to express H19 or H19-targeting short hairpin RNA (shRNA), or their respective controls, at a multiplicity of infection of 1:100. H19 expression was determined by reverse transcription-quantitative PCR. Hypoxic injury was induced and assessed by analyzing the level of apoptosis, the cell cycle distribution and the mitochondrial membrane potential using flow cytometry in the different groups. The expression of the PI3K/AKT and the ERK/p38 signaling pathways were analyzed using western blotting. It was found that hypoxia stimulated apoptosis, induced G1 phase cell cycle arrest and increased the mitochondrial depolarization rate in H9c2 cells. When compared with the hypoxic model group, the H19 overexpression group had a significantly reduced rate of apoptosis (P=0.016), a smaller G1 population and a higher S phase population (P=0.018 and P=0.031, respectively), and a reduced mitochondrial depolarization rate (P=0.036). By contrast, the H19 shRNA group exhibited the opposite trends, suggesting that hypoxia-induced injury was alleviated by the overexpression of H19 and was aggravated by the knockdown of H19. The present mechanistic studies revealed that H19 may decrease hypoxia-induced cell injury by activating the PI3K/AKT and ERK/p38 pathways. The results of the present study suggested that H19 may alleviate hypoxia-induced myocardial cell injury through the activation of the PI3K/AKT and ERK/p38 pathways.

Correspondence to: Dr Guohai Xu, Department of Anesthesiology, The Second Affiliated Hospital of Nanchang University, 1 Minde Road, East Lake, Nanchang, Jiangxi 330006, P.R. China
E-mail: xuguohai1221@163.com

Dr Yanhua Tang, Department of Cardiac Surgery, The Second Affiliated Hospital of Nanchang University, 1 Minde Road, East Lake, Nanchang, Jiangxi 330006, P.R. China
E-mail: yanhuatang@126.com

*Contributed equally

Key words: long non-coding RNA H19, myocardial ischemia/reperfusion injury, knockdown, PI3K/AKT, mitogen-activated protein kinase

Introduction

Cardiovascular disease is one of the leading causes of death worldwide (1). During cardiac surgery, myocardial ischemia/reperfusion (I/R) injury often leads to adverse cardiovascular outcomes, including acute heart failure due to severe hypoxia (2). Multiple signaling pathways are involved in protective mechanisms against myocardial I/R injury, including the PI3K/AKT and the mitogen-activated protein kinase (MAPK) signaling pathways. The PI3K/AKT pathway is an important intracellular signaling pathway for the regulation of the cell cycle. Previous studies have suggested that the PI3K/AKT signaling pathway mediates a protection mechanism against myocardial I/R injury in rats (3,4). Inhibition of the cardiac p38-MAPK pathway has been reported to delay ischemic cell death and protect cardiac mitochondria from I/R injury (5,6).

Long non-coding RNAs (lncRNAs) are a class of non-coding RNA molecule with a length of >200 nucleotides. lncRNAs represent the most prevalent class of non-coding RNA, with the majority of the human genome transcribed into lncRNAs (7). lncRNAs can act as important regulators in a number of biological processes, including stem cell lineage differentiation (8), cancer development and metastasis (9,10) and angiogenesis (11,12). The lncRNA H19 (H19) is located on human chromosome 11 and expresses a 2.3 kb lncRNA transcribed from the maternal inherited allele (13). Increased expression of H19 was detected in rats following surgically induced myocardial I/R, suggesting that H19 may have a role in the protective mechanisms against I/R injury (14). Previous studies have also indicated that H19 exerts protective effects against hypoxia-induced injury in cardiomyocytes (15,16).

Nevertheless, to date, the functional role of H19 in myocardial hypoxic injury has not been fully elucidated. The present study aimed to investigate the effects and the molecular mechanism of H19 in response to hypoxia-induced I/R injury using a myocardial cell model.

Materials and methods

Cell lines and culture. The rat cardiomyoblast cell line, H9c2, and 293T cells were purchased from BeNa Culture Collection. Cells were maintained in DMEM (Hyclone; GE Healthcare Life Sciences) containing 10% FBS (Gibco; Thermo Fisher Scientific, Inc.), 100 U/ml penicillin and 100 μg/ml streptomycin at 37˚C and 5% CO_2 in an incubator.

Design and construction of H19 expressing/silencing lentivirus. To construct an H19 expressing lentiviral vector, the H19 cDNA sequence (NR_002196.2) was synthesized by Sangon Biotech Co., Ltd. and cloned into the pLVX-Puro vector following the Lentivector User Manual (Takara Bio, Inc.). The following PCR reaction mixture was used: 25 μl 2x Super Pfx MasterMix (Beijing CoWin Biotech Co., Ltd.), 2.5 μl 10 μM forward primer, 2.5 μl 10 μM reverse primer, 2.0 μl DNA template, 18 μl ddH_2O. The PCR was performed as follows: 98˚C for 1 min, 30 cycles of 98˚C for 5 sec, 58˚C for 30 sec, and 72˚C for 30 sec, followed by 72˚C for 5 min. The pLVX-Puro vector was used as a negative control. To construct an H19 silencing lentiviral vector, the following oligonucleotides encoding a short hairpin RNA (shRNA) against H19 were designed and synthesized by Genscript and cloned into the pGreenPuro™ vector (Addgene, Inc.): Sense, 5'-GATCCTGAATATGCTGCACTTTACAACTCGAGTTGTAAAGTGCAGCATATTCATTTTTG-3' and antisense, 5'-AATTCAAAAAATGAATATGCTGCACTTTACAACTCGAGTTGTAAAGTGCAGCATATTCAG-3'. The positive-sense and antisense strands harboring *Bam*H and *Eco*R digestion sites annealed to form a double-stranded structure, which was then cloned into the pGreenPuro plasmid. The lentiviral vector containing a non-silencing sequence was used as a negative control. The sequence of constructs was confirmed by PCR and Sanger sequencing.

To package lentiviruses, 293T packaging cells were plated in a 10 cm plate. At 70% confluency, the cells were co-transfected with 2.5 μg of the appropriate lentiviral vector (pLVX-Puro-H19 vector, pLVX-Puro vector, pGreenPuro™ shH19 vector or pGreenPuro™ non-silencing vector), 5 μg of psPAX and 5 μg of pMD2G (Addgene, Inc.) using a Lipofectamine® 3000 transfection kit (Invitrogen; Thermo Fisher Scientific, Inc.). The viral supernatants were harvested after 48 h and filtered with a 0.45 μm filter. The titer of the lentivirus was determined using a lentivirus titration kit (Applied Biological Materials), following the manufacturer's instructions.

Cell culture and infection. H9c2 cells were cultured in 6-well plates and divided into six groups: Normal control, model control, H19 expression, blank expression, H19 interference and blank interference groups. Cells in the H19 expression, blank expression, H19 interference and blank interference groups were infected with H19 overexpression, blank expression, H19-targeting shRNA and blank interference lentiviruses, respectively, at a multiplicity of infection of 1:100. Cells in the normal control group were then cultured under normoxia (21% O_2, 5% CO_2 and 74% N2). Cells in all other groups were incubated in an incubator containing 94% N_2, 5% CO_2 and 1% O_2 to stimulate hypoxia injury. After 48 h, cells in each group were collected and subjected to subsequent analyses.

Apoptosis assay. At 48 h after transfection, apoptosis was determined using a FITC Annexin V Apoptosis Detection kit I (BD Biosciences). Briefly, cells were resuspended in 1X binding buffer, stained with 5 μl FITC Annexin V (BD Biosciences) and 10 μl of propidium iodide (PI; BD Biosciences) in the dark for 10 min. The fluorescence of cells was detected using a NovoCyte 2060R flow cytometer (ACEA Biosciences, Inc.) at 488 nm within 1 h and analyzed using NovoExpress software version 1.3.0 (ACEA Biosciences, Inc.).

Measurement of mitochondrial membrane potential. At 48 h after transfection, the mitochondrial membrane potential of cells was determined using a JC-1 mitochondrial membrane potential assay kit (Abcam). Briefly, cells were resuspended in 500 μl of 1X incubation buffer and stained with 1 μl JC-1 at 37˚C, 5% CO_2 for 10 min. Cells were collected by centrifugation at 420 x g at room temperature for 5 min and washed twice with 1X incubation buffer. The fluorescence of cells was analyzed using a NovoCyte 2060R flow cytometer (ACEA Biosciences, Inc.) at 488 nm within 1 h and analyzed using NovoExpress software version 1.3.0 (ACEA Biosciences, Inc.).

Cell cycle analysis. At 48 h after transfection, the cell cycle was analyzed using flow cytometry. Briefly, cells were fixed with 70% ethanol for 24 h at 4˚C and stained with 100 μl of PI (30 ng/ml) for 30 min at 37˚C in the dark. The percentage of the population in G1, S or G2/M phase was analyzed using a NovoCyte 2060R flow cytometer (ACEA Biosciences, Inc.) at 488 nm within 1 h and analyzed using NovoExpress software version 1.3.0 (ACEA Biosciences, Inc.).

Western blot analysis. Cells were collected at 48 h after transfection. Total protein was extracted using RIPA lysis buffer (Beijing CoWin Biotech Co., Ltd.) and quantified using bicinchoninic acid protein assay kit (Beijing CoWin Biotech Co., Ltd.). Protein extracts (60 μg) were separated by SDS-PAGE using 10% gels and transferred onto PVDF membranes. The membranes were blocked with 5% skim milk for 30 min at room temperature and incubated overnight at 4˚C with the following antibodies: β-actin (1:2,000; cat. no. TA-09; OriGene Technologies, Inc.), AKT (1:2,000; cat. no. bs-0115R; BIOSS), ERK1/2 (1:1,000; cat. no. bs-0022R; BIOSS), p38 (1:2,000; cat. no. bs-0637R; BIOSS), PI3K (1:2,000; cat. no. ab191606; Abcam), phosphorylated (p-)AKT (1:1,000; cat. no. ab38449; Abcam), p-p38 (1:1,000; cat. no. ab47363; Abcam), p-ERK1/2 (1:1,000; cat. no. ab214362; Abcam) and p-PI3K (1:1,000; cat. no. ab127617; Abcam). The membranes were washed with PBS and incubated with horseradish peroxidase-conjugated goat anti-mouse (1:2,000; cat. no. ZB-2305; OriGene Technologies, Inc.) or anti-rabbit (1:2,000; cat. no. ZB-2305; OriGene Technologies, Inc.) secondary antibodies for 2 h at room temperature. Protein bands were visualized using an

ECL Western blotting detection system (GE Healthcare). The relative expression of proteins was quantified using ImageJ software version 1.52e (National Institutes of Health) with β-actin used as the internal control.

Reverse transcription-quantitative PCR (RT-qPCR). Cells were collected 48 h after transfection. Total RNA was extracted using TRIzol reagent (Invitrogen; Thermo Fisher Scientific, Inc.) and reverse transcribed into cDNA using SuperScript II (Invitrogen; Thermo Fisher Scientific, Inc.) at 42˚C. qPCR was performed using UltraSYBR mixture (Takara Biotechnology Co., Ltd.) in an ABI 7500 System (Applied Biosystems; Thermo Fisher Scientific, Inc.). The reactions conditions were as follows: 95˚C for 10 min followed by 40 cycles of 95˚C for 10 sec, 58˚C for 30 sec and 72˚C for 30 sec. The following primers were synthesized by Invitrogen (Thermo Fisher Scientific, Inc.) and used in the PCR: H19 forward, 5'-GTG GGACACTGCCGTAGAA-3' and reverse, 5'-CAGGAAAGG AGGAAGAAGAAAA-3'; and U6 forward, 5'-CTCGCTTCG GCAGCACA-3' and reverse, 5'-AACGCTTCACGAATTTGC GT-3'. Data was analyzed using the $2^{-\Delta\Delta Cq}$ method (17). The relative expression of lncRNA H19 was calculated using U6 as the internal control.

Statistical analysis. All experiments were performed in triplicate. Data are presented as the mean ± SD and were analyzed using SPSS 19.0 software (IBM Corp.). Differences among groups were compared using one-way ANOVA followed by Tukey's post-hoc test. Ratios were compared using the χ^2 tests. P<0.05 was considered to indicate a statistically significant difference.

Results

Hypoxia-induced apoptosis is alleviated by H19 overexpression and is aggravated by H19 interference. The expression of H19 in all groups was determined using RT-qPCR. As shown in Fig. 1, the model control, blank expression, blank interference and normal control groups had a similar level of H19 expression (all P>0.05). H19 expression was significantly increased in the H19 expression group (P=0.015) and significantly reduced in the H19 interference group (P=0.023) compared with the model control group. As shown in Fig. 2, the rate of apoptosis in the model group was significantly higher than in normal control group (P=0.021), indicative of hypoxia-induced myocardial cell injury. The rate of apoptosis was significantly reduced in the H19 expression group (P=0.016) and was significantly increased in the H19 interference group compared with the model group (P=0.022). The blank expression and blank interference groups had similar rates of apoptosis as the model group (both P>0.05).

Hypoxia-induced G1 phase cell cycle arrest is attenuated by H19 overexpression and is aggravated by H19 interference. The cell cycle distribution was analyzed using flow cytometry. As shown in Fig. 3, the proportion of H9c2 cells in the G1 phase in the model group was significantly higher compared with the normal control group (P=0.020) and the percentage of S phase cells was significantly lower (P=0.043), suggesting that hypoxia induced a G1 phase cell cycle arrest. The H19 expression and normal control groups had a similar proportion of H9c2 cells in G1 phase (P>0.05). The H19 interference group had a significantly higher G1 population compared with the normal control group (P=0.012). When compared with the model group, the H19 expression group had a significantly lower G1 and a higher S phase population (P=0.018 and 0.031, respectively), whereas the H19 interference group had a significantly higher G1 population and a smaller S phase population (P=0.029 and 0.045, respectively). The G1 and S phase populations in the blank expression and blank interference groups were similar to the model group (all P>0.05).

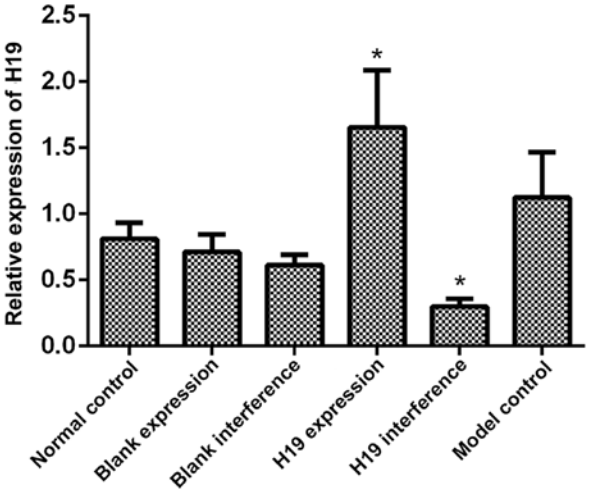

Figure 1. Reverse transcription-quantitative PCR analysis of H19 expression in the different groups. Cells in the normal control group were cultured under normoxia. Cells in the model control and different infection groups (blank expression, H19 expression, H19 interference and blank interference) were collected after 48 h of culture in hypoxic conditions. The model control, blank expression, blank interference and normal control groups had a similar level of H19 expression (all P>0.05). H19 expression was significantly increased in the H19 expression group (P=0.015) and significantly reduced in the H19 interference group (P=0.023) compared with the model control group. Data were analyzed using the $2^{-\Delta\Delta Cq}$ method. The relative expression of H19 was calculated using U6 as the internal control. All samples were measured in triplicate. *P<0.05 vs. model group. H19, long non-coding RNA H19.

Hypoxia-induced mitochondrial membrane depolarization is reduced by H19 overexpression, but is enhanced by H19 interference. Under hypoxic treatment, the depolarization rate of the mitochondrial membrane potential in the model group was increased compared with the normal control group (P=0.033; Fig. 4). The mitochondrial depolarization rate was significantly reduced in the H19 expression group (P=0.036) and was increased in the H19 interference group (P=0.012) compared with the model group. By contrast, the blank expression and blank interference groups had similar depolarization rates as the model group (both P>0.05).

PI3K/AKT and ERK/p38 pathways are activated by H19 overexpression, but are inhibited by H19 interference. The underlying mechanism for the H19-asssociated regulation of apoptosis, the cell cycle and mitochondrial membrane potential was analyzed by western blotting. The results showed that the levels of p-PI3K, p-AKT and p-p38 in the model group were higher compared with the normal control group (all P>0.05). p-ERK1/2 expression was significantly lower in the

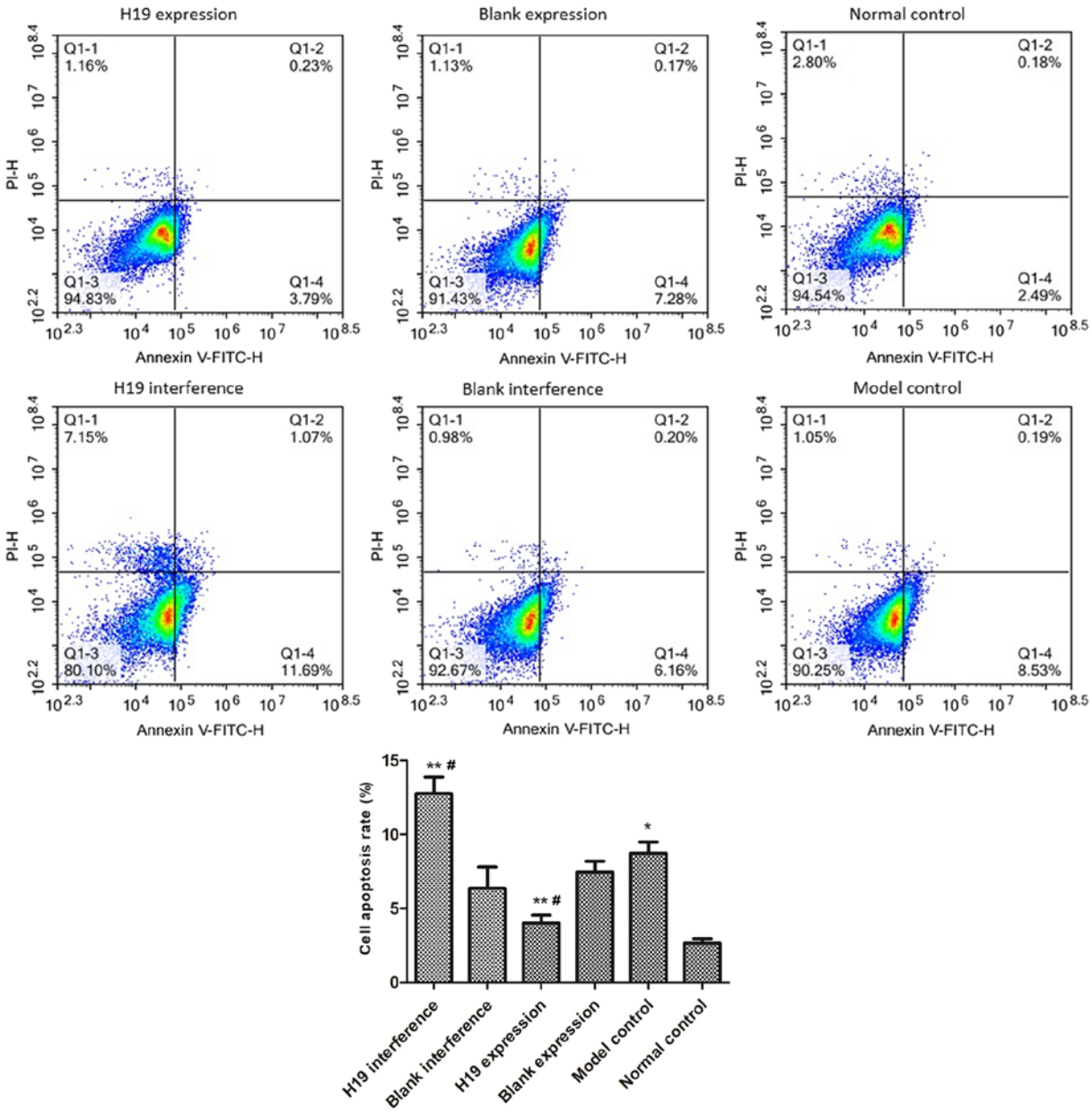

Figure 2. Hypoxia-induced H9c2 apoptosis is aggravated by H19 knockdown and is alleviated by H19 overexpression. Cells in the normal control group were cultured under normoxia. Cells in the model control and different infection groups (H19 expression, blank expression, H19 interference and blank interference) were collected after 48 h of culture in hypoxic conditions. The level of apoptosis was determined using flow cytometry. All samples were measured in triplicate. *P<0.05, **P<0.01 vs. normal group; $^{\#}$P<0.05 vs. model group. H19, long non-coding RNA H19; PI, propidium iodide.

model group compared with the normal control (P<0.05). The overexpression of H19 increased the levels of p-PI3K, p-ERK1/2 and p-p38 compared with the model group (all P<0.05). p-AKT level in the H19 overexpression group was similar as compared to the model group (P>0.05). The effects of H19 interference were the opposite to H19 overexpression in regulating the expression of p-p38 and p-PIK3 (all P<0.05, Fig. 5). H19 interference also significantly reduced the p-AKT expression as compared to model group (P<0.05). H19 interference and model groups had similar p-ERK1/2 expression (P>0.05). These findings indicated that the overexpression of H19 may attenuate hypoxia-induced cell injury by regulating the PI3K/AKT and ERK/p38 pathways. Nevertheless, it is worth noting that there are some variation among the model and blank expression/interference groups, indicating that some other pathways may also be involved in the H19 regulatory process.

Discussion

Hypoxia is commonly used to induce a myocardial cell injury model (18). In the present study, H9c2 cells were exposed to hypoxic conditions to induce cell injury. As a result, these cells exhibited an increased level of apoptosis, G1 cell cycle arrest and depolarization of the mitochondrial membrane potential. The role of H19 has been previously studied in several cancers; however, its role remains controversial. For instance, H19 overexpression has been reported to enhance carcinogenesis and metastasis in gastric cancer (19). Contrary to this, it was found that H19 does not affect the proliferation or cell cycle

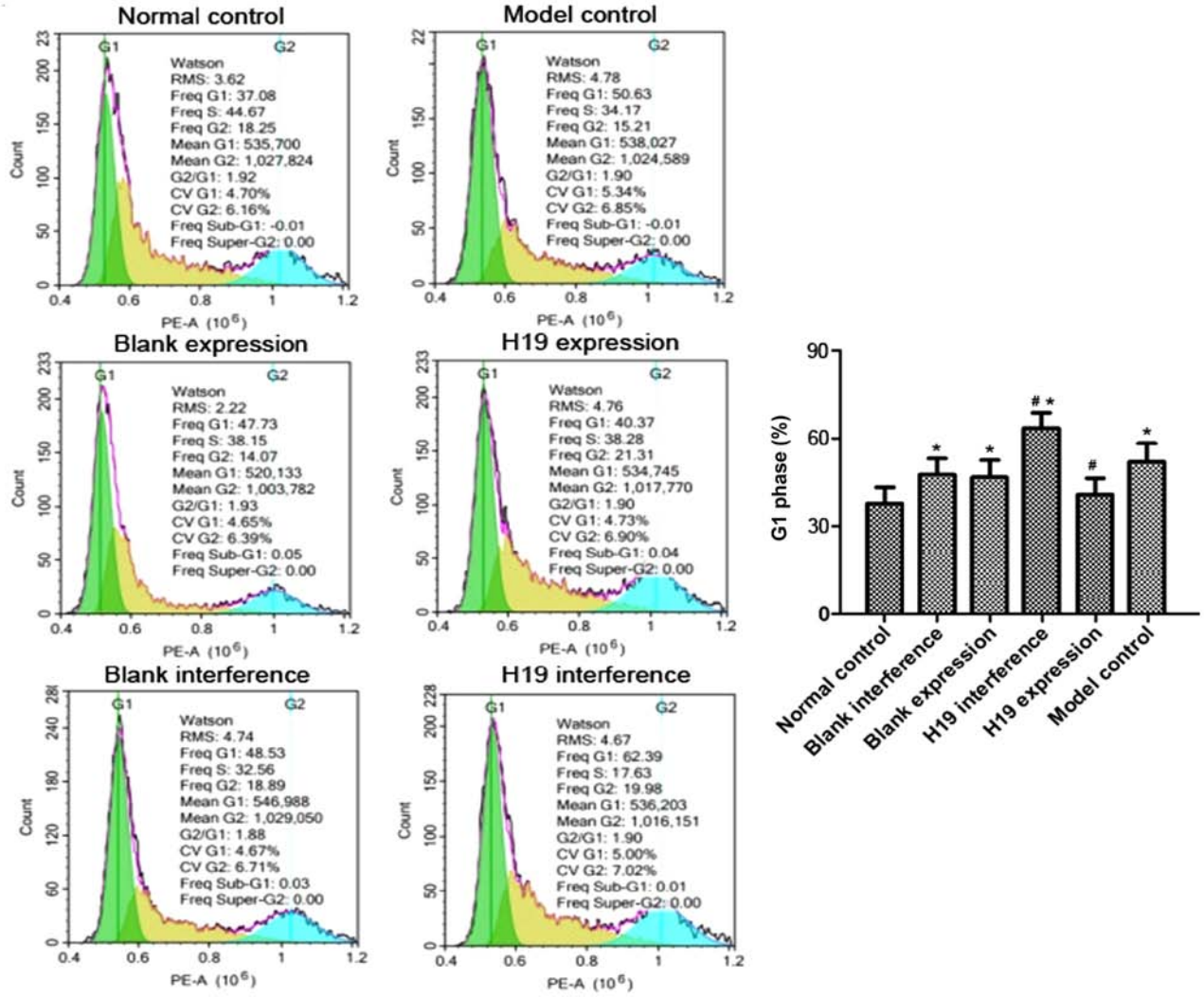

Figure 3. Flow cytometry analysis of the cell cycle distribution of H9c2 cells. Cells in the normal control group were cultured under normoxia. Cells in the model control and different infection groups (H19 expression, blank expression, H19 interference and blank interference) were collected after 48 h of culture in hypoxic conditions. The percentage of cells in the G1 phase was quantified. All samples were measured in triplicate. *P<0.05 vs. normal group; #P<0.05 vs. model group. PE, phycoerythrin; RMS, root mean square; Freq, frequency; CV, coefficient of variation; H19, long non-coding RNA H19.

distribution of breast cancer cells (20). There are few studies reporting the effects of H19 in hypoxia-injured myocardial cells (16). In the present study, H19 expression was found to be increased in hypoxia-treated cells, suggesting the possible involvement of H19 in protection against hypoxia-induced cell injury. H9c2 cells were transfected with H19 expressing or silencing lentiviruses to investigate the role of H19 in hypoxia-injured cells. It was found that H19 overexpression alleviated hypoxia-induced injury mediated apoptosis, cell cycle arrest and mitochondrial membrane potential depolarization; however, these processes were aggravated by H19 knockdown. These results suggested that H19 attenuated hypoxia-induced myocardial cell injury, which is consistent with previous studies (15,16). The findings of this previous report (16) and the present study are consistent with each other in regard to the molecular mechanism of H19 in protecting against myocardial I/R injury. Nevertheless, it is worth noting that the two studies have different experimental designs. Specifically, the present study examined the role of H19 regulation on the cell cycle and mitochondrial changes in cells in addition to cell apoptosis, which more directly reveals the cellular/intracellular responses during the process of myocardial I/R injury, whereas the reference only examined the cell behavior, including cell viability, migration and apoptosis.

The PI3K/AKT signal pathway is an important pathway for protecting myocardial cells against hypoxia-induced injury (21,22). Xiao *et al* (23) reported that hydrogen sulfide protects myocardial cells against hypoxia-induced injury via mTOR activation. Chen *et al* (24) reported that lipoxin A4-induced heme oxygenase-1 protects cardiomyocytes against hypoxia/reoxygenation injury via p38 MAPK activation and the nuclear factor erythroid 2-related/antioxidant responsive element complex. IT has been previously reported that AKT activation reduces myocardial cell apoptosis by upregulating the expression of Bcl-2 (25). The relationship between the Bcl-2 family proteins and mitochondria-mediated apoptosis pathway is well-established (26). Thus, it is speculated that H19 may regulate mitochondrial apoptosis by activating the PI3K/AKT/mTOR pathway. In the present study the effects of H19 on mitochondrial membrane potential

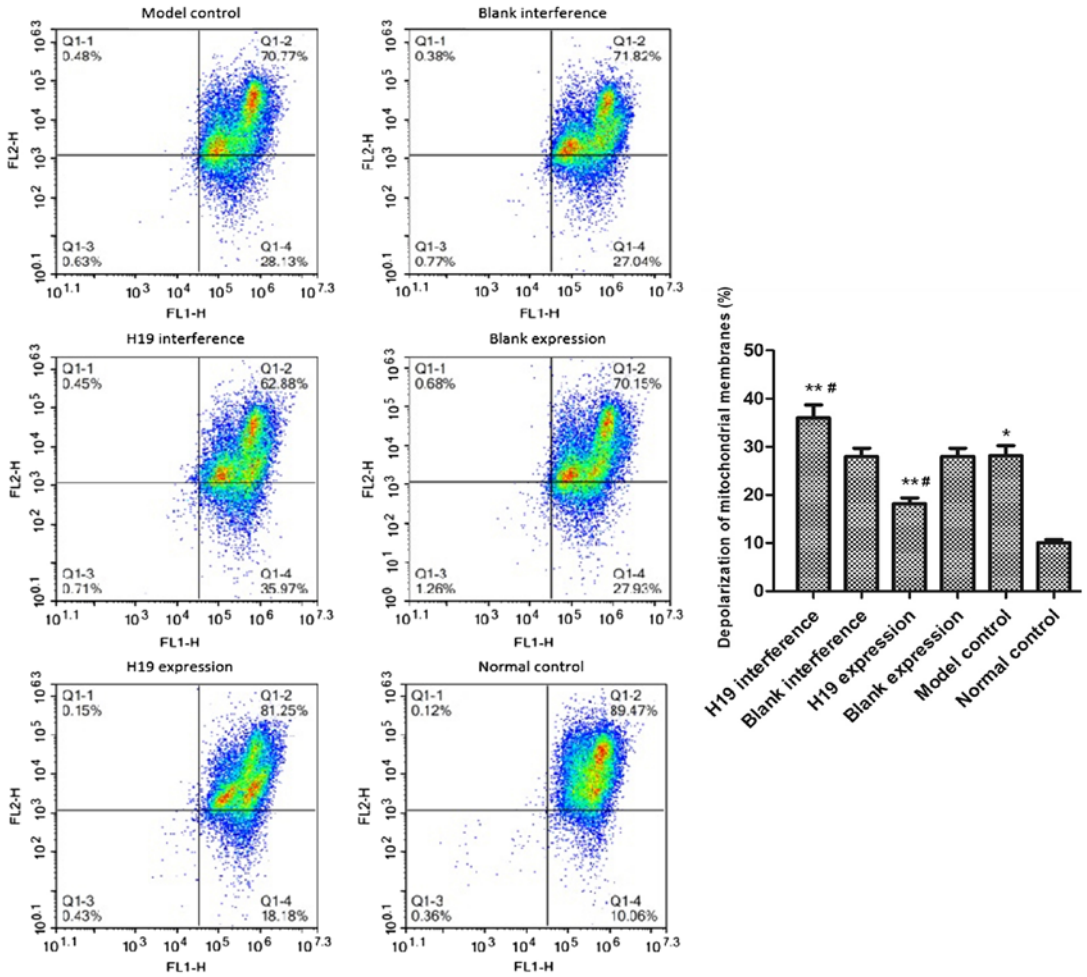

Figure 4. Hypoxia-induced mitochondrial membrane depolarization is reduced by H19 overexpression and is enhanced by H19 interference. Cells in normal control group were cultured under normoxia. Cells in the model control and different infection groups (H19 expression, blank expression, H19 interference and blank interference) were collected after 48 h of culture in hypoxic conditions. The mitochondrial depolarization rate was determined using flow cytometry. All samples were measured in triplicate. *P<0.05, **P<0.01 vs. normal group; $^{\#}$P<0.05 vs. model group. H19, long non-coding RNA H19; FL, fluorescence.

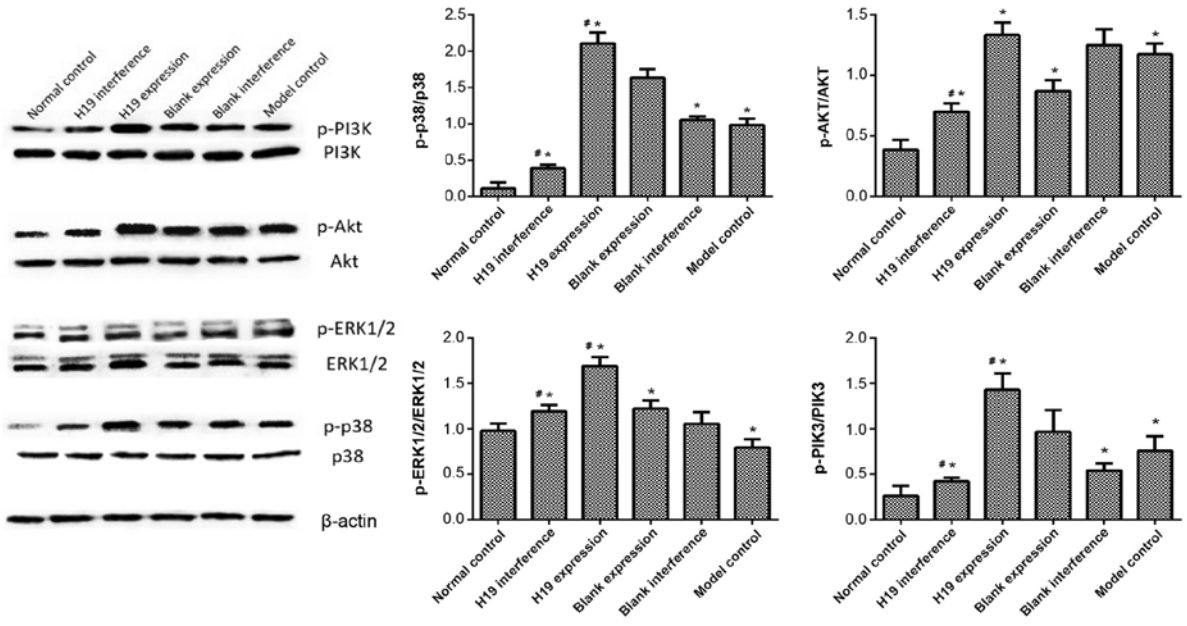

Figure 5. PI3K/AKT and ERK/p38 pathways were regulated by H19. Cells in the normal control group were cultured under normoxia. Cells in the model control and different infection groups (H19 expression, blank expression, H19 interference and blank interference) were collected after 48 h of culture in hypoxic conditions. The expression levels of p-PI3K, p-AKT, p-ERK1/2, p-p38, PI3K, AKT, ERK1/2 and p38 were determined using western blotting with β-actin as the internal control. All samples were measured in triplicate. *P<0.05 vs. normal group; $^{\#}$P<0.05 vs. model group. H19, long non-coding RNA H19; p-, phosphorylated.

were assessed, as was the activation of the PI3K/AKT/mTOR signaling pathway and MAPK activation, in order to elucidate the mechanisms underlying the possible protective effects of H19 against hypoxia-induced cell injury. It was demonstrated that the overexpression of H19 stabilized the mitochondrial membrane potential and upregulated the PI3K/AKT/mTOR pathway in hypoxia-treated H9c2 cells, while H19 interference had the opposite effect, indicating that H19 alleviated hypoxia-induced cell injury by reducing the mitochondrial apoptosis pathway and activating the PI3K/AKT and MAPK pathways.

In conclusion, the present study demonstrated that the overexpression of H19 decreased hypoxia-induced cell injury by increasing cell viability and decreasing apoptosis, whereas knockdown of H19 had the opposite effects. Furthermore, it was found that the overexpression of H19 may protect H9c2 cells from hypoxia-induced injury by activating the PI3K/AKT/mTOR and MAPK pathways. The present study may provide new insights into the prevention and treatment of acute myocardial infarction. Nevertheless, the present study was limited by the use of only one cell line. Future experiments should be conducted with other types of cardiomyocytes (for example, AC16 human cardiomyocyte and HCFB human cardiac fibroblasts) to verify the findings of the present study. Additionally, in-depth mechanistic studies should be performed to further elucidate the protective effects of H19. Findings from future studies should also be verified in animal models.

Acknowledgements

Not applicable.

Funding

No funding was received.

Availability of data and materials

The datasets used and/or analyzed during the present study are available from the corresponding author on reasonable request.

Authors' contributions

LiY performed the majority of experiments and drafted the paper. LeY, JZ, ZZ and CL helped with experiments. BZ and XH analyzed the data and drafted part of the paper. GX and YT conceived the study, supervised the experiments and edited the manuscript.

Ethics approval and consent to participate

Not applicable.

Patient consent for publication

Not applicable.

Competing interests

The authors declare that they have no competing interests.

References

1. Mc Namara K, Alzubaidi H and Jackson JK: Cardiovascular disease as a leading cause of death: How are pharmacists getting involved? Integr Pharm Res Pract 8: 1-11, 2019.
2. Hearse DJ and Bolli R: Reperfusion induced injury: Manifestations, mechanisms, and clinical relevance. Cardiovasc Res 26: 101-108, 1992.
3. Yu LN, Yu J, Zhang FJ, Yang MJ, Ding TT, Wang JK, He W, Fang T, Chen G and Yan M: Sevoflurane postconditioning reduces myocardial reperfusion injury in rat isolated hearts via activation of PI3K/Akt signaling and modulation of Bcl-2 family proteins. J Zhejiang Univ Sci B 11: 661-672, 2010.
4. Chen Q, Xu T, Li D, Pan D, Wu P, Luo Y, Ma Y and Liu Y: JNK/PI3K/Akt signaling pathway is involved in myocardial ischemia/reperfusion injury in diabetic rats: Effects of salvianolic acid A intervention. Am J Transl Res 8: 2534-2548, 2016.
5. Zhao MM, Yang JY, Wang XB, Tang CS, Du JB and Jin HF: The PI3K/Akt pathway mediates the protection of SO(2) preconditioning against myocardial ischemia/reperfusion injury in rats. Acta Pharmacol Sin 34: 501-506, 2013.
6. Vassalli G, Milano G and Moccetti T: Role of mitogen-activated protein kinases in myocardial ischemia-reperfusion injury during heart transplantation. J Transplant 2012: 928954, 2012.
7. Furuno M, Pang KC, Ninomiya N, Fukuda S, Frith MC, Bult C, Kai C, Kawai J, Carninci P, Hayashizaki Y, *et al*: Clusters of internally primed transcripts reveal novel long noncoding RNAs. PLoS Genet 2: e37, 2006.
8. Hou J, Zhou C, Long H, Zheng S, Guo T, Wu Q, Wu H, Zhong T and Wang T: Long noncoding RNAs: Novel molecules in cardiovascular biology, disease and regeneration. Exp Mol Pathol 100: 493-501, 2016.
9. Li L, Feng T, Lian Y, Zhang G, Garen A and Song X: Role of human noncoding RNAs in the control of tumorigenesis. Proc Natl Acad Sci USA 106: 12956-12961, 2009.
10. Whitehead J, Pandey GK and Kanduri C: Regulation of the mammalian epigenome by long noncoding RNAs. Biochim Biophys Acta 1790: 936-947, 2009.
11. Kumar MM and Goyal R: LncRNA as a therapeutic target for angiogenesis. Curr Top Med Chem 17: 1750-1757, 2017.
12. Zhao J, Du P, Cui P, Qin Y, Hu C, Wu J, Zhou Z, Zhang W, Qin L and Huang G: LncRNA PVT1 promotes angiogenesis via activating the STAT3/VEGFA axis in gastric cancer. Oncogene 37: 4094-4109, 2018.
13. Gabory A, Jammes H and Dandolo L: The H19 locus: Role of an imprinted non-coding RNA in growth and development. Bioessays 32: 473-480, 2010.
14. Rajagopalan V, Zhang Y, Pol C, Costello C, Seitter S, Lehto A, Savinova OV, Chen YF and Gerdes AM: Modified low-dose triiodo-L-thyronine therapy safely improves function following myocardial ischemia-reperfusion injury. Front Physiol 8: 225, 2017.
15. Zhang X, Cheng L, Xu L, Zhang Y, Yang Y, Fu Q, Mi W and Li H: The Lncrna, H19 mediates the protective effect of hypoxia postconditioning against hypoxia-reoxygenation injury to senescent cardiomyocytes by targeting microRNA-29b-3p. Shock 52: 249-256, 2019.
16. Livak KJ and Schmittgen TD: Analysis of relative gene expression data using real-time quantitative PCR and the 2(-Delta Delta C(T)) method. Methods 25: 402-408, 2001.
17. Zhu HM and Deng L: Evaluation of cardiomyocyte hypoxia injury models for the pharmacological study in vitro. Pharm Biol 50: 167-174, 2012.
18. Gong LC, Xu HM, Guo GL, Zhang T, Shi JW and Chang C: Long non-coding RNA H19 protects H9c2 cells against hypoxia-induced injury by targeting microRNA-139. Cell Physiol Biochem 44: 857-869, 2017.
19. Li H, Yu B, Li J, Su L, Yan M, Zhu Z and Liu B: Overexpression of lncRNA H19 enhances carcinogenesis and metastasis of gastric cancer. Oncotarget 5: 2318-2329, 2014.
20. Lottin S, Adriaenssens E, Dupressoir T, Berteaux N, Montpellier C, Coll J, Dugimont T and Curgy JJ: Overexpression of an ectopic H19 gene enhances the tumorigenic properties of breast cancer cells. Carcinogenesis 23: 1885-1895, 2002.
21. Li C, Tian J, Li G, Jiang W, Xing Y, Hou J, Zhu H, Xu H, Zhang G, Liu Z and Ye Z: Asperosaponin VI protects cardiac myocytes from hypoxia-induced apoptosis via activation of the PI3K/Akt and CREB pathways. Eur J Pharmacol 649: 100-107, 2010.

22. Lin KH, Kuo WW, Jiang AZ, Pai P, Lin JY, Chen WK, Day CH, Shen CY, Padma VV and Huang CY: Tetramethylpyrazine ameliorated hypoxia-induced myocardial cell apoptosis via HIF-1α/JNK/p38 and IGFBP3/BNIP3 inhibition to upregulate PI3K/Akt survival signaling. Cell Physiol Biochem 36: 334-344, 2015.
23. Xiao J, Zhu X, Kang B, Xu J, Wu L, Hong J, Zhang Y, Ni X and Wang Z: Hydrogen sulfide attenuates myocardial hypoxia-reoxygenation injury by inhibiting autophagy via mTOR activation. Cell Physiol Biochem 37: 2444-2453, 2015.
24. Chen XQ, Wu SH, Zhou Y and Tang YR: Lipoxin A4-induced heme oxygenase-1 protects cardiomyocytes against hypoxia/reoxygenation injury via p38 MAPK activation and Nrf2/ARE complex. PLoS One 8: e67120, 2013.
25. Wang B, Shravah J, Luo H, Raedschelders K, Chen DD and Ansley DM: Propofol protects against hydrogen peroxide-induced injury in cardiac H9c2 cells via Akt activation and Bcl-2 up-regulation. Biochem Biophys Res Commun 389: 105-111, 2009.
26. Edlich F: BCL-2 proteins and apoptosis: Recent insights and unknowns. Biochem Biophys Res Commun 500: 26-34, 2018.